DeepML: Deep LSTM for Indoor Localization with Smartphone Magnetic and Light Sensors

Xuyu Wang, Zhitao Yu, and Shiwen Mao
Department of Electrical and Computer Engineering, Auburn University, Auburn, AL 36849-5201
Email: {xzw0029, zzy0021}@auburn.edu, smao@ieee.org

***Abstract*—With the fast increasing demands of location-based service and proliferation of smartphones and other mobile devices, accurate indoor localization has attracted great interest. In this paper, we present DeepML, a deep long short-term memory (LSTM) based system for indoor localization using the smartphone magnetic and light sensors. We verify the feasibility of using bimodal magnetic and light data for indoor localization through experiments. We then design the DeepML system, which first builds bimodal images by data preprocessing, and then trains a deep LSTM network to extract the location features. Newly received magnetic field and light intensity data is then exploited for estimating the location of the mobile device using an improved probabilistic method. Our extensive experiments verify the effectiveness of the proposed DeepML system.**

***Index Terms*—Bimodal data; deep learning; deep long short-term memory (LSTM); indoor localization; light intensity; magnetic field.**

I. Introduction

Indoor localization has been a research hotspot for decades [1]. However, unlike outdoor GPS navigation systems, there are still no robust indoor localization systems widely adopted by now. In fact, people still cannot use the popular Google Maps to navigate to a meeting room in an unfamiliar office building. Recently, there is considerable new interest in indoor localization techniques, driven by the proliferation of smartphones and other mobile devices, which, on one hand, makes it possible to enable many location based services, and on the other hand, provides an array of embedded sensors that can be exploited for indoor localization. Specifically, many researchers focus on WiFi [2] based fingerprinting indoor localization using received signal strength (RSS) [3], [4] or Channel State information (CSI) [5]–[11]. These methods can achieve robust meter-level accuracy but cannot work effectively when the WiFi signal is weak or not available in some scenarios, such as underground parking areas.

In contrast, the geomagnetic field is *omnipresent* and thus can be considered as a ubiquitous signature for indoor localization. In the past, geomagnetism basically needs to be used with special equipments for robot tracking [12] and navigation [13]. In [13], researchers employ the leader-follower model in a navigation system, where customized magnetic sensing devices are used for blind people. On the other hand, for magnetic field based localization with smartphones, the authors in [14] use mobile phones to measure magnetic field intensity and use them as magnetic signatures for identifying locations and rooms. However, according to its strategy, this system depends heavily on pillars in the building and only achieves room-level accuracy. Recently, the Magicol system combines magnetism and WiFi RSSI to build a fingerprint map, which is designed with a particle-filtering based inertial measurement unit (IMU) engine for localization and tracking [15]. Other systems based on magnetic sequences matching are proposed for improving tracking accuracy [16]. The above magnetic field based, smartphone localization systems require the user to walk around for data collection and online localization.

In addition, visible light is also omnipresent and has been exploited for localization, due to the density and stability of lighting infrastructures. For example, visible light intensity in an underground park area usually does not change over time, and is not influenced by the outdoor sunlight, which can be thus leveraged for indoor localization. Existing visible light localization systems, such as polarized LEDs [17] and collocated LEDs [18], require customized LED drivers to emit identity beacons, which increases the system cost. To eliminate the need for customized LEDs, LiTell system [19] extracts high-frequency features from fluorescent light for localization. Other visible light localization systems for smartphones are based on particle-filtering and light intensity data sequence, for which there is still room for improvement by exploiting movement sensors [20], [21].

In this paper, we exploit bimodal magnetic field and ambient light data for indoor localization with a deep learning approach. The proposed scheme is motivated by the following observations. First, the magnetic field and light intensity at each location are highly stable and robust over time. Second, magnetic field and light intensity are complementary to each other at many locations. For example, magnetic field does not perform well at some locations, while these locations may have different light intensities, which can be used to distinguish them. Using the bimodal data can enhance magnetic field based indoor localization schemes. Third, using bimodal data with magnetic field and light intensity can increase the size of input data, thus improving location diversity and recognition performance. Moreover, we incorporate a deep long-short term memory (LSTM) network to train the bimodal data, which is a popular recurrent neural network (RNN) to deal with long-range dependencies [22], [23]. The deep LSTM network has been successfully employed for speech recognition [24] and human activity recognition [25]. Compared to conventional fingerprinting based methods, the deep LSTM network only requires one group of weights trained for all training locations,

instead of creating a database for each training location. This feature can accelerate location prediction and reduce the data storage requirement.

In particular, we design DeepML, a **Deep** LSTM network based indoor localization system using smartphone **M**agnetic and **L**ight sensors. The proposed DeepML system includes a data preprocessing module for collecting magnetic field and light intensity data, and to create bimodal image data with a sliding window method. DeepML also has an offline training phase that includes feature extraction, the deep LSTM network, and a softmax classifier. A fully connected layer is implemented for extracting features from bimodal image data. The deep LSTM network consists of two layers of LSTM networks to achieve a stonger learning and representation ability. The softmax classifier employs the cross-entropy to measure the difference between true labeled data and the normalized output data, as well as the L2 regularization hyper-parameter to avoid over-fitting. The back propagation through time (BPTT) algorithm, which is a gradient-based technique for training certain types of RNNs, is used for training the deep LSTM network. For online location prediction, an improved probabilistic method is leveraged for estimating the location of the target smartphone using newly received magnetic field and light intensity data.

The main contributions of this paper include:

- We experimentally validate the feasibility of using magnetic field and light intensity data for indoor localization. We show that both data are stable over time, and the fusion of magnetic field and light intensity data can improve location diversity and accuracy. To the best of our knowledge, this is the first work to employ bimodal magnetic field and light intensity data for indoor localization with a deep LSTM network approach.
- We present the DeepML system design, which first builds bimodal images to train the deep LSTM network, and then employs newly received magnetic field and light data for estimating the location of the target mobile device.
- We implement the proposed DeepML system with Android smartphones, and validate its performance in two typical indoor environments with extensive experiments. DeepML outperforms the baseline scheme that uses magnetic field data only with considerable gains in all the experiments.

In the remainder of the paper, we present the preliminaries and motivation in Section II. We describe the DeepML design in Section III and our performance evaluation in Section IV. Section V concludes this paper.

II. Preliminaries and Motivation

In this section, we examine the characteristic of magnetic field and light intensity data, especially on their stability and location diversity. Then, we show how to fuse magnetic field and light intensity data for detection of location features.

A. Magnetic Field Preliminaries

The magnetic field of the earth, i.e., the geomagnetic field, is ubiquitous on the surface of the earth, with magnitude ranging from 0.25 to 0.65 Gauss. The magnetometer in most smartphones can measure the magnetic field, in the form of a vector with three elements (m_x, m_y, m_z), which describes the magnetic field component for north, east, and vertical directions, respectively. For studying the stability and location diversity of magnetic field data, we measure the magnetic field data (m_x, m_y, m_z) at 10 different locations selected in a corridor of 20 meters long in the Broun Hall on Auburn University Campus. We obtain five different datasets collected at five different times. Fig. 1 shows the magnetic field data components (m_x, m_y, m_z) for different locations and times. We find that for any fixed location, all the three elements (m_x, m_y, m_z) exhibit small variations over time, as indicated by the negligible error bars. This validates the stability of magnetic field data with respect to location, which can guarantee the reliability of fingerprinting based indoor localization using magnetic field data.

In addition, we also find good diversity of magnetic field data for different locations. In Fig. 1, the magnetic field data exhibits sufficient variations for different locations. For example, each of the three elements (m_x, m_y, m_z) has different values for locations 1 and 2. Specifically, we can see that at least one element of the magnetic field data changes for a different location. The indoor magnetic field has local anomalies (or, local disturbances), because modern buildings generally have many ferromagnetic structures. The ambient magnetic field leads to geomagnetic anomalies, which can be leveraged for accurate indoor localization.

B. Light Intensity Preliminaries

Modern buildings usually use several types of light bulbs, such as the compact fluorescent lamp (CFL) and light-emitting diode (LED) [26]. Most smartphones can capture light intensity from such bulbs. In fact, light propagates in the air from the light bulbs to the smartphone light receiver, with different radiant intensity measurements for different locations, which are susceptible to the indoor propagation environment, such as shadowing, scattering, and reflection for different surfaces. This motivates the work on light intensity based fingerprinting localization technique [27].

To study the stability and location diversity of light intensity at different times and locations, we measure the light intensities at 10 different locations in the same corridor, and collected five datasets at different times. Fig. 2 presents the characteristics of light intensity data at different locations and times. Similarly, we find light intensity data is quite stable for any given location, as indicated by the negligible error bars. Furthermore, light intensity measurements take different values for some different locations, e.g., see neighboring locations 1 and 2, 4 and 5, and 9 and 10. But for some other neighboring locations, e.g., 3 and 4, and 7 and 8, the light intensity values are very close. Thus, unlike magnetic field

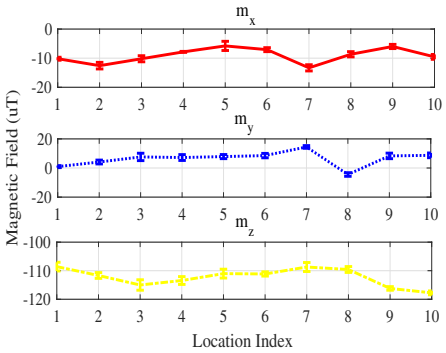

Fig. 1. Characteristics of magnetic field data.

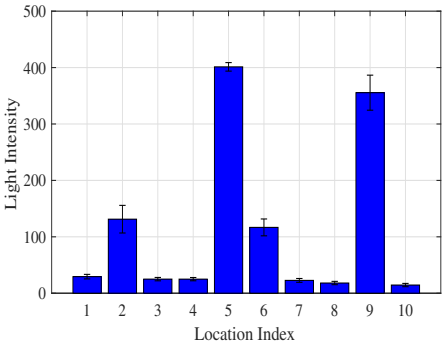

Fig. 2. Characteristics of light intensity data.

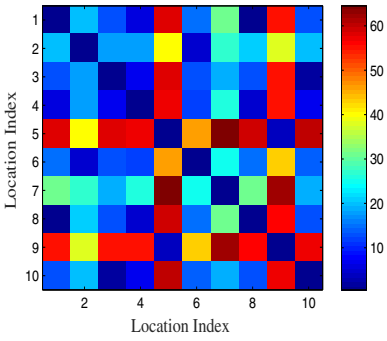

Fig. 3. Confusion matrix of the bimodal data with magnetic field vector and light intensity.

data, it is difficult to use light intensities only as fingerprints for indoor localization.

C. Fusion of Magnetic Field Data and Light Intensity

Our measurement study of magnetic field and light intensity motivates us to use them as bimodal data for indoor localization. This is because we can use the different light intensities at different locations to improve the accuracy of magnetic field based indoor localization. By fusing the magnetic field and light intensity data, the dimension of input data is increased, making it suitable for the proposed deep LSTM based scheme, to strengthen the uniqueness of location features.

To measure the location diversity of the bimodal data with magnetic field and light intensity, we define the confusion matrix for N different locations as

$$\boldsymbol{D} = \begin{bmatrix} d_{11} & d_{12} & d_{13} & \dots & d_{1N} \\ d_{21} & d_{22} & d_{23} & \dots & d_{2N} \\ \vdots & \vdots & \vdots & \ddots & \vdots \\ d_{N1} & d_{N2} & d_{N3} & \dots & d_{NN} \end{bmatrix}, \quad (1)$$

where d_{ij} denotes the Euclidean distance between the two signal vectors of locations i and j, which can be computed by $d_{ij} = ||S_i - S_j||_2$, where S_i is the signal vector of location i, including both the magnetic field vector and light intensity. To measure the performance of different datasets, we need to normalize the confusion matrix with the same metric.

Fig. 3 presents the confusion matrix of the bimodal data with magnetic field vector and light intensity for an experiment with 10 locations in the corridor. We can see that the fusion of magnetic field and light intensity achieves great location diversity with large distances for most location pairs, which is different from using magnetic field vector only or light intensity only in Sections II-A and II-B. Such enhanced diversity is highly desirable for the training and location estimation of the proposed deep LSTM network for indoor localization.

III. The Proposed DeepML System

A. DeepML System Architecture

We design the DeepML system and prototype it with a Samsung Galaxy S7 Edge smartphone with an Android 7.0 platform. The Android application is developed with Android Studio 2.3.3 for data collection and preprocessing. The proposed DeepML system employs both magnetic field data and ambient light for two main reasons. First, as discussed in Section II, the variance in magnetic field and light intensity at each location is generally very small; they are both highly stable over time for each given position. Second, magnetic field measurements may not show sufficient location diversity in some areas. Incorporating the bimodal data could exploit the different light intensities for enhanced location diversity for such areas. Magnetic field and light intensity are complementary to each other for many locations. Using the bimodal data can improve the localization performance.

The design of DeepML is presented in Fig. 4. The most salient features include the use of bimodal magnetic and light data, and the deep LSTM network used for extracting location features from the bimodal data. DeepML first performs *data preprocessing* of collected magnetic field and light data, to build bimodal images using a sliding window method. During the *offline training* phase, we implement feature extraction for the bimodal images for effectively training the deep LSTM network. Compared to conventional fingerprinting based methods, DeepML does not need to establish a database for each training location, where either raw data or extracted features are stored as fingerprints. Rather, our DeepML system only requires one group of weights to be trained for all training locations. In the *online testing* phase, we incorporate an improved probabilistic approach for location estimation, based on newly received magnetic and light bimodal data from the target mobile device.

B. Data Preprocessing

We first collect and record real-time readings from the smartphone magnetic field ambient light sensors. Due to the sequence size requirement of the deep LSTM network, we need to reduce the sampling rate of the magnetic field sensor, to make its readings in-sync with that from the ambient light sensor. Specifically, we obtain 1500 rows of magnetic field and light intensity combined patterns for each training location. For example, the size of training data is about 15000 rows for the 10 training locations in the corridor, and 18000 rows for the 12 train locations in the laboratory scenario. For online

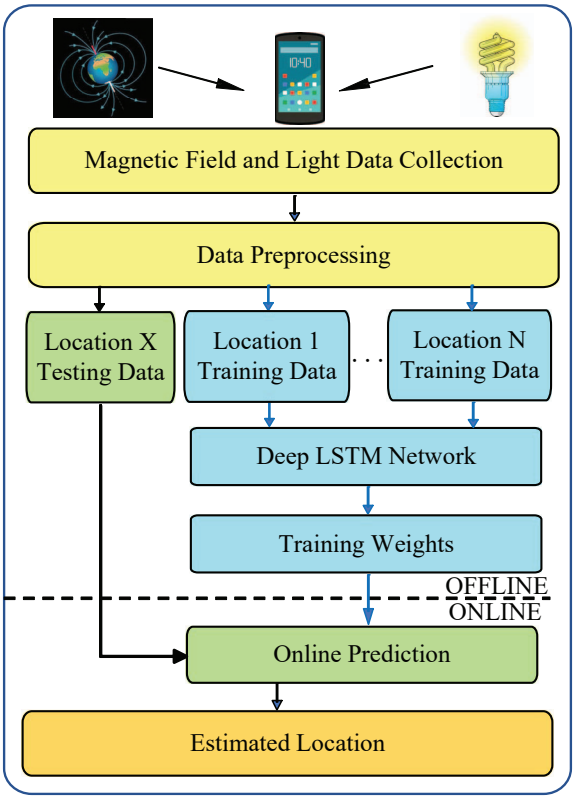

Fig. 4. The DeepML system architecture.

location estimation, the data size is about 400 rows for each test location.

We next employ a sliding window to build bimodal image data. For both training and testing phases, we set the size of the sliding window to 20. Thus, we can obtain the bimodal image data with size 20 $\times$ 4, with 20 measured data points in the column dimension and 4 feature values in the row dimension, including m_x, m_y, m_z for magnetic field and l for light.

C. Offline Training

For offline training, we propose a deep LSTM approach to extract location features from the bimodal image data with magnetic field and light intensity. The offline training module includes feature extraction, the deep LSTM network, and the Softmax classifier.

1) Feature Extraction: For better feature extraction, we implement one fully connected layer for extracting features from raw magnetic fields and light intensity data, which is formulated as

$$z_t = \text{ReLU}(W x_t + b), \tag{2}$$

where x_t and z_t are the input and output of the fully connected layer, respectively, W and b are the weights and biases of the fully connected layer, respectively. ReLU$(\cdot)$ is the *rectified linear unit*, which is considered as the activation function with ReLU$(x) = \max(x, 0)$. The ReLU$(\cdot)$ function has several advantages such as sparse representations, efficient gradient propagation and computation.

2) Deep LSTM Network: After feature extraction, we next use the deep LSTM algorithm for training optimal weights, where the LSTM network is a popular recurrent neural network (RNN) that can effectively deal with long-range dependency [22], [23]. It can solve the problems of exploding or vanishing gradients found in RNNs. Moreover, LSTM can exploit temporal information of magnetic field and light intensity data through recursively mapping the input sequence to output label by using the hidden LSTM units. Each LSTM unit has a built-in memory cell to store information over time using non-linear gate units, which can control the change of values and memory contents. For the proposed DeepML system, we stack two layers of the LSTM network to obtain a stronger learning and representation ability for magnetic and light sensor data, thus improving the localization performance.

3) Softmax Classifier: The output of the final cell's hidden state in the second LSTM network is the input to a fully connected layer, which uses a basic neural network with one hidden layer to train the output data using the *Softmax classifier*. Moreover, the input data to the Softmax function is in the form of a N dimensional vector $q = [q_1, q_2, ..., q_N]$, where N is the number of training locations. The ith input data can be obtained as $q_i = h_f^T w_i$, where h_f is the output vector of the final cell's hidden state in the second LSTM network, and w_i is the weight vector of the fully connected layer. The Softmax function then maps the N dimensional vector to normalized data $p = [p_1, p_2, ..., p_N]$, that is

$$p_i = \frac{e^{q_i}}{\sum_{n=1}^{N} e^{q_n}} = \frac{e^{h_f^T w_i}}{\sum_{n=1}^{N} e^{h_f^T w_n}}, \quad \text{for } i = 1, 2, ..., N. \tag{3}$$

Let $J(\theta)$ be the *loss function* with the weight parameter θ. We adopt the *cross-entropy* to measure the difference between the true labeled data and the normalized output data, and use the L2 regularization hyperparameter to avoid over-fitting. To obtain the optimal weights, the training loss is minimized as

$$\min_{\theta} J(\theta) = -\sum_{i=1}^{N} y_i \log(p_i) + \frac{\lambda}{2} \|\theta\|_2^2, \tag{4}$$

where y_i denotes the true labeled data for the ith location, and λ is the L2 regularization hyperparameter. We then train the parameters in the deep LSTM using Backpropagation Through Time (BPTT) of LSTM. We also use the Adam Optimizer for improving the efficiency of optimization [28].

D. Online Location Estimation

For online location test, we first build M bimodal images with magnetic and light sensor data (as shown in the data preprocessing section), each of which has the same size as training images. Then, we leverage a probabilistic method for estimating the location of the target mobile device by feeding the M bimodal images to the trained deep LSTM network.

Let $\boldsymbol{\omega}$ denote the output results of the Softmax classifier using the deep LSTM network for N training locations with

M newly measured bimodal images. We have

$$\boldsymbol{\omega} = \begin{bmatrix} \omega_{11} & \omega_{12} & \omega_{13} & \dots & \omega_{1M} \\ \omega_{21} & \omega_{22} & \omega_{23} & \dots & \omega_{2M} \\ \vdots & \vdots & \vdots & \ddots & \vdots \\ \omega_{N1} & \omega_{N2} & \omega_{N3} & \dots & \omega_{NM} \end{bmatrix}. \quad (5)$$

We then compute the average result for M output data at every location, thus reducing the variance of the output results. Let $\bar{\omega}_n$ be the mean of the output data vector $[\omega_{n1}, \omega_{n2}, ..., \omega_{nM}]$ in the nth row. The mean vector can be obtained as $\bar{\omega} = [\bar{\omega}_1, \bar{\omega}_2, ..., \bar{\omega}_N]$.

Finally, the position of the target mobile device is estimated as a weighted average of all the N training locations, as

$$\hat{L} = \sum_{i=1}^{N} l_n \times \bar{\omega}_n, \quad (6)$$

where l_n is the nth training location.

IV. Experimental Study

A. Experiment Setup

We prototype the DeepML system with a Samsung Galaxy S7 Edge smartphone on the Android 7.0 platform. Moreover, we implement an Android application with Android Studio 2.3.3 for data collection and preprocessing. We compare DeepML with a benchmark that uses magnetic field data only. To guarantee a fair comparison, we use for these two approaches the same magnetic field dataset and the same deep LSTM parameters to estimate the location of the mobile device. We experiment with the two methods in two different indoor scenarios.

- *Lab Scenario:* This is a 6×12 m^2 computer laboratory in Broun Hall on the Auburn University campus. The lab is a cluttered environment with tables, chairs, and computers. The floor plan is shown in Fig. 5. We choose 12 training locations, which are marked as red squares. The distance between two neighboring training locations is 1.6 m. We collect 1800 rows of light intensity and magnetic field combined pattern for each training location, and 400 rows of data for each test location. Note that each test location is different from the known training locations.
- *Corridor Scenario:* This is a 2.4 × 20 m^2 corridor in Broun Hall. As shown in Fig. 6, we employ 10 training locations along a straight line with 1.6 m separation. The training data size is 1500 rows and the testing data size is 400 rows.

For online test, we leverage an LSTM deep leaning model using Tensorflow on a computer with CPU 4720HQ and then integrate it with the data collection Android application, which achieves localization estimation in real-time.

B. Localization Performance

Figure 7 plots the cumulative distribution function (CDF) of localization errors of the two schemes in the lab experiment. For this environment with complex light intensity and magnetic field distribution, DeepML is able to leverage bimodal magnetic-light features to predict location accurately. Fig. 7 shows that about 58% of the location errors with the

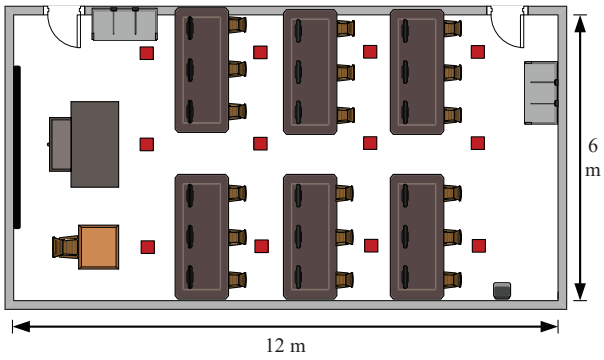

Fig. 5. Layout of the computer lab scenario: training locations are marked as red squares.

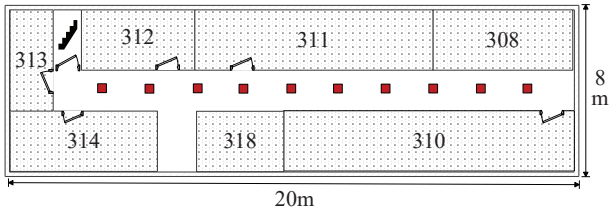

Fig. 6. Layout of the corridor scenario: training locations are marked as red squares.

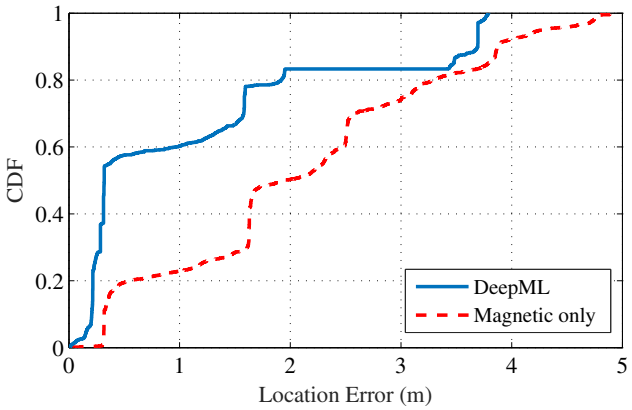

Fig. 7. CDF of localization error of the lab experiment.

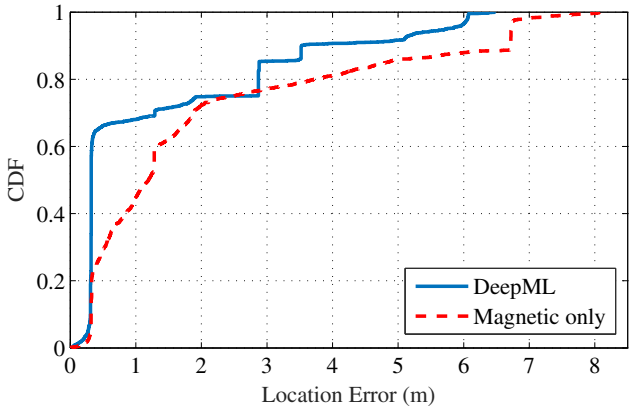

Fig. 8. CDF of localization error of the corridor experiment.

proposed DeepML system are under 0.5 m, while 20% of the location errors with the magnetic field only scheme are under 0.5 m. Moreover, DeepML has 82% of the test locations with location errors less than or equal to 2 m, while it is 50% for the magnetic field only scheme. DeepML achieves a maximum error of 3.7 m, which is much better than the 5 m maximum error of the benchmark scheme. Apparently, the proposed DeepML system is more accurate for the cluttered lab environment.

Fig. 8 presents the CDF of localization errors of both schemes in the corridor scenario. There are about 65% of the test locations that have an estimation error less than or equal to 0.4 m for DeepML, while it is 25% for the magnetic only scheme. Additionally, we find DeepML has 87% of the test locations achieving an error under 3 m, comparing to 78% of the magnetic only scheme. Moreover, for the corridor scenario, the maximum location errors for DeepML and the magnetic only scheme are 6.5 m and 8.2 m, respectively. The proposed DeepML system is more robust than the baseline scheme.

The experiments validate that DeepML outperforms the benchmark scheme in both experiment scenarios. The main reason is that dual-module fingerprint has stronger location diversity, which carries more location features. In many cases magnetic field data and light intensity are complementary to each other. Furthermore, the proposed deep LSTM network can effectively extract the rich location features from the bimodal data, to achieve enhanced localization performance.

V. Conclusions

In this paper, we presented DeepML, a deep LSTM based system for indoor localization using the magnetic and light sensors in smartphones. We first experimentally verified the feasibility of using the magnetic-light bimodal data for indoor localization. We then presented the DeepML design, with its data preprocessing, deep LSTM network, and probabilistic location estimation modules. Our experiments under two representative indoor environments demonstrated the effectiveness of the proposed DeepML system.

Acknowledgment

This work is supported in part by the US NSF under Grant CNS-1702957, and by the Wireless Engineering Research and Education Center (WEREC) at Auburn University.

References

[1] Y. Gu, A. Lo, and I. Niemegeers, "A survey of indoor positioning systems for wireless personal networks," *IEEE Commun. Surveys Tuts.*, vol. 11, no. 1, pp. 13–32, Jan. 2009.

[2] M. Gong, B. Hart, and S. Mao, "Advanced wireless LAN technologies: IEEE 802.11ac and beyond," *ACM Mobile Computing and Communications Review (MC2R)*, vol. 18, no. 4, pp. 48–52, Oct. 2014.

[3] P. Bahl and V. N. Padmanabhan, "Radar: An in-building RF-based user location and tracking system," in *Proc. IEEE INFOCOM'00*, Tel Aviv, Israel, Mar. 2000, pp. 775–784.

[4] M. Youssef and A. Agrawala, "The Horus WLAN location determination system," in *Proc. ACM MobiSys'05*, Seattle, WA, June 2005, pp. 205–218.

[5] J. Xiao, K. Wu., Y. Yi, and L. Ni, "FIFS: Fine-grained indoor fingerprinting system," in *Proc. IEEE ICCCN'12*, Munich, Germany, Aug. 2012, pp. 1–7.

[6] X. Wang, L. Gao, and S. Mao, "CSI phase fingerprinting for indoor localization with a deep learning approach," *IEEE Internet of Things Journal*, vol. 3, no. 6, pp. 1113–1123, Dec. 2016.

[7] X. Wang, L. Gao, S. Mao, and S. Pandey, "CSI-based fingerprinting for indoor localization: A deep learning approach," *IEEE Trans Veh. Technol.*, vol. 66, no. 1, pp. 763–776, Jan. 2017.

[8] X. Wang, L. Gao, and S. Mao, "BiLoc: Bi-modality deep learning for indoor localization with 5GHz commodity Wi-Fi," *IEEE Access Journal*, vol. 5, no. 1, pp. 4209–4220, Mar. 2017.

[9] X. Wang, X. Wang, and S. Mao, "CiFi: Deep convolutional neural networks for indoor localization with 5GHz Wi-Fi," in *Proc. IEEE ICC 2017*, Paris, France, May 2017, pp. 1–6.

[10] X. Wang, L. Gao, S. Mao, and S. Pandey, "DeepFi: Deep learning for indoor fingerprinting using channel state information," in *Proc. WCNC'15*, New Orleans, LA, Mar. 2015, pp. 1666–1671.

[11] X. Wang, X. Wang, and S. Mao, "ResLoc: Deep residual sharing learning for indoor localization with CSI tensors," in *Proc. IEEE PIMRC 2017*, Montreal, Canada, Oct. 2017.

[12] J. Chung, M. Donahoe, C. Schmandt, I.-J. Kim, P. Razavai, and M. Wiseman, "Indoor location sensing using geo-magnetism," in *Proc. ACM MobiSys'11*, Bethesda, MD, June/July 2011, pp. 141–154.

[13] W. Storms, J. Shockley, and J. Raquet, "Magnetic field navigation in an indoor environment," in *Proc. IEEE UPINLBS'10*. Kirkkonummi, Finland: IEEE, Oct. 2010, pp. 1–10.

[14] B. Gozick, K. P. Subbu, R. Dantu, and T. Maeshiro, "Magnetic maps for indoor navigation," *IEEE Trans. Instrum. Meas.*, vol. 60, no. 12, pp. 3883–3891, Dec. 2011.

[15] Y. Shu, C. Bo, G. Shen, C. Zhao, L. Li, and F. Zhao, "Magicol: Indoor localization using pervasive magnetic field and opportunistic WiFi sensing," *IEEE J. Sel. Areas Commun.*, vol. 33, no. 7, pp. 1443–1457, July 2015.

[16] Y. Ma, Z. Dou, Q. Jiang, and Z. Hou, "Basmag: An optimized HMM-based localization system using backward sequences matching algorithm exploiting geomagnetic information," *IEEE Sensors J.*, vol. 16, no. 20, pp. 7472–7482, Oct. 2016.

[17] Z. Yang, Z. Wang, J. Zhang, C. Huang, and Q. Zhang, "Wearables can afford: Light-weight indoor positioning with visible light," in *Proc. ACM. MobiSys'15*, Florence, Italy, May 2015, pp. 317–330.

[18] Y.-S. Kuo, P. Pannuto, K.-J. Hsiao, and P. Dutta, "Luxapose: Indoor positioning with mobile phones and visible light," in *Proc. ACM MobiCom'14*, Maui, HI, Sept. 2014, pp. 447–458.

[19] C. Zhang and X. Zhang, "LiTell: Robust indoor localization using unmodified light fixtures," in *Proc. ACM MobiCom'16*, New York City, NY, Oct. 2016, pp. 230–242.

[20] Q. Xu, R. Zheng, and S. Hranilovic, "IDyLL: Indoor localization using inertial and light sensors on smartphones," in *Proc. ACM UbiComp'15*. Osaka, Japan: ACM, Sept. 2015, pp. 307–318.

[21] Z. Zhao, J. Wang, X. Zhao, C. Peng, Q. Guo, and B. Wu, "NaviLight: Indoor localization and navigation under arbitrary lights," in *Proc. IEEE INFOCOM'17*. Atlanta, GA: IEEE, May 2017, pp. 1–9.

[22] F. A. Gers, J. Schmidhuber, and F. Cummins, "Learning to forget: Continual prediction with lstm," *J. Neural Comput.*, vol. 12, no. 10, pp. 2451–2471, Oct. 2000.

[23] K. Greff, R. K. Srivastava, J. Koutník, B. R. Steunebrink, and J. Schmidhuber, "Lstm: A search space odyssey," *IEEE Trans. Neural Netw. Learn. Syst.*, vol. 28, no. 10, pp. 2222–2232, 2017.

[24] A. Graves, N. Jaitly, and A.-r. Mohamed, "Hybrid speech recognition with deep bidirectional LSTM," in *Proc. IEEE ASRU'13*, Olomouc, Czech Republic, Dec. 2013, pp. 273–278.

[25] F. J. Ordonez and D. Roggen, "Deep convolutional and LSTM recurrent neural networks for multimodal wearable activity recognition," *MDPI Sensors*, vol. 16, no. 1, p. 115, Jan. 2016.

[26] T.-H. Do and M. Yoo, "An in-depth survey of visible light communication based positioning systems," *MPDI Sensors*, vol. 16, no. 5, p. 678, May 2016.

[27] J. Randall, O. Amft, J. Bohn, and M. Burri, "LuxTrace: Indoor positioning using building illumination," *Springer Person. ubi. comput.*, vol. 11, no. 6, pp. 417–428, Aug. 2007.

[28] D. Kingma and J. Ba, "Adam: A method for stochastic optimization," *arXiv preprint arXiv:1412.6980*, 2014, [online] Available: https://arxiv.org/abs/1412.6980.